CELL BIOLOGY

High-throughput small molecule screening reveals Nrf2-dependent and -independent pathways of cellular stress resistance

David B. Lombard[1,2]*, William J. Kohler[1], Angela H. Guo[1], Christi Gendron[3], Melissa Han[1], Weiqiao Ding[4], Yang Lyu[3], Tsui-Ting Ching[5], Feng-Yung Wang[6], Tuhin S. Chakraborty[3], Zaneta Nikolovska-Coleska[1], Yuzhu Duan[7], Thomas Girke[7], Ao-Lin Hsu[3,4,8], Scott D. Pletcher[2,3], Richard A. Miller[1,2]

Aging is the dominant risk factor for most chronic diseases. Development of antiaging interventions offers the promise of preventing many such illnesses simultaneously. Cellular stress resistance is an evolutionarily conserved feature of longevity. Here, we identify compounds that induced resistance to the superoxide generator paraquat (PQ), the heavy metal cadmium (Cd), and the DNA alkylator methyl methanesulfonate (MMS). Some rescue compounds conferred resistance to a single stressor, while others provoked multiplex resistance. Induction of stress resistance in fibroblasts was predictive of longevity extension in a published large-scale longevity screen in *Caenorhabditis elegans*, although not in testing performed in worms and flies with a more restricted set of compounds. Transcriptomic analysis and genetic studies implicated Nrf2/SKN-1 signaling in stress resistance provided by two protective compounds, cardamonin and AEG 3482. Small molecules identified in this work may represent attractive tools to elucidate mechanisms of stress resistance in mammalian cells.

INTRODUCTION

Aging is the key risk factor for most chronic debilitating diseases, conditions that impose great human suffering and ever-increasing health care costs in industrialized societies (*1*). Genetic studies suggest that some of the pathways that govern the rate of aging and the onset of age-related disease in model organisms—particularly insulin/insulin growth factor–like and mechanistic target of rapamycin (mTOR) signaling—may function similarly in humans to limit healthy lifespan. A large body of evidence has demonstrated that the aging rate can be markedly slowed in invertebrates and in rodents (*2*). Mice subjected to dietary restriction or with certain single gene mutations live much longer than controls (*2*). Studies by the Interventions Testing Program (ITP) and others have shown that specific small molecules, such as rapamycin, acarbose, canagliflozin, and 17α-estradiol, can substantially extend mouse lifespan (https://nia.nih.gov/research/dab/interventions-testing-program-itp). In these studies, experimental animals typically remain healthy even late in life, with a much-reduced disease burden compared to controls. Thus, drugs with antiaging activity can delay or abrogate many age-associated pathologies.

To date, all compounds that delay aging in mammals have been identified by testing based on prior knowledge of mechanism of action and/or data generated in invertebrate models rather than via unbiased screening approaches. Unfortunately, the major vertebrate model used in aging biology, *Mus musculus*, has a lifespan of nearly 3 years, presenting a prohibitive barrier to large-scale direct screening for antiaging effects using lifespan as an end point. The most extensive effort to identify compounds with antiaging activity in mice, the ITP, cannot test more than a handful of agents each year. Thus, although rodent studies have conclusively proven that extension of mammalian lifespan by small molecules is possible, currently, only a handful of drugs with robust and replicable lifespan benefits, i.e., >10% extension, have been identified.

To circumvent this challenge, several groups have performed screens in more tractable, short-lived invertebrate model organisms to identify small molecules that increase lifespan. The first such large-scale screen, performed in the nematode *Caenorhabditis elegans*, revealed that certain serotonin signaling inhibitors extend longevity in this organism (*3*). Other screens have revealed the ability of anticonvulsants (*4*), angiotensin-converting enzyme antagonists (*5*), and modulators of other signaling pathways to increase worm lifespan (*6*). Recent studies have used in silico strategies to prioritize compounds for direct lifespan testing in nematodes and other organisms (*7*, *8*).

An alternative and complementary strategy to these approaches is to evaluate test compounds in mouse or human cells using phenotypes that serve as surrogates for organismal lifespan. In this regard, cellular resistance to environmental stress is a frequent correlate of longevity (*9*). In mammals, dermal fibroblasts derived from longer-lived species or from long-lived mouse mutants show resistance to some forms of lethal injury (*10*–*12*). Similarly, in *C. elegans*, many long-lived mutants show resistance to a variety of environmental insults (*13*), including oxidative stress, a phenotype that has been used to screen for these mutants (*14*). An analogous strategy, based on screens for surrogate stress resistance endpoints, has been used to identify long-lived mutants in budding yeast (*15*). A group of compounds that promote lifespan extension in worms was enriched for molecules that protect against oxidative stress (*6*).

We performed high-throughput screening (HTS) to identify small molecules that induce resistance against multiple forms of cellular injury in mouse skin fibroblasts. Three screens were performed in

[1]Department of Pathology, University of Michigan, Ann Arbor, MI, USA. [2]Geriatrics Center, University of Michigan, Ann Arbor, MI, USA. [3]Department of Molecular and Integrative Physiology, University of Michigan, Ann Arbor, MI, USA. [4]Department of Internal Medicine, Division of Geriatric and Palliative Medicine, University of Michigan, Ann Arbor, MI, USA. [5]Institute of Biopharmaceutical Sciences, National Yang Ming University, Taipei 112, Taiwan. [6]Institute of Biochemistry and Molecular Biology, National Yang Ming University, Taipei 112, Taiwan. [7]Institute for Integrative Genome Biology, University of California Riverside, Riverside, CA, USA. [8]Research Center for Healthy Aging, China Medical University, Taichung, Taiwan.
*Corresponding author. Email: davidlom@med.umich.edu

parallel based on resistance to the superoxide generator paraquat (PQ), the heavy metal cadmium (Cd), and the DNA alkylating agent methyl methanesulfonate (MMS). Mechanistic studies implicated Nrf2/SKN-1 signaling in stress resistance provoked by two hits, cardamonin and AEG 3482. Hits identified in these studies may warrant further study to provide new insights into mechanisms of stress resistance in mammalian cells. In addition, because many of our hit compounds are U.S. Food and Drug Administration–approved drugs with favorable safety profiles, the agents that induce stress resistance in our screens may warrant further testing in mice for health and longevity benefits.

RESULTS

HTS identifies small molecules that induce resistance against multiple stressors in mammalian fibroblasts

We performed HTS using mouse tail fibroblasts (MTFs). Stress resistance of this cell type correlates with organismal longevity in mouse strains in which single gene mutations extend healthy lifespan (*9*). We initially defined the basic parameters for cell-based stress assays using MTFs, optimizing growth media, seeding density, and incubation time. Using these parameters, we then performed an extensive series of pilot experiments using the cellular stressors PQ, MMS, and Cd, along with selected candidate chemical rescue agents (curcumin and arsenite), to optimize conditions for HTS for induction of stress resistance (fig. S1, A to C). In these pilot studies, we tested a wide range of stressor concentrations for PQ (0.2 to 10 μM), MMS (0.1 to 2 mM), and Cd (0.2 to 10 μM).

Using these optimized conditions, we then evaluated small-molecule libraries containing a total of 6351 compounds (Biofocus NCC, MicroSource Spectrum 2400, Prestwick, LOPAC (Library of Pharmacologically Active Compounds), and a focused collection), including some duplicates included in more than one library, for ability to protect MTFs from cell death induced by PQ at a single dose, 16 μM (table S1). In total, >4500 unique compounds were screened. A typical assay is shown, in which 640 candidate rescue agents were tested (Fig. 1A). Many compounds within this particular set protected cells against PQ toxicity. Testing of duplicate plates of rescue compounds revealed low plate-to-plate variation (fig. S1D). Similar primary screens were conducted using Cd and MMS as stressors (table S1).

To facilitate comparisons between experiments and among the different stressors, we calculated an adjusted score for each compound, compensating for minor batch variation so that each test day's dataset shared a common median value (table S1, see Materials and Methods for details). In brief, to determine the adjusted raw score, we calculated the natural log (ln) of [relative light units (RLU)/1000] for each test compound. The ln(RLU/1000) scores were then slightly adjusted so that each day's experiment had identical median ln(RLU/1000) scores. Histograms of the $\log_{10}$ values of these adjusted raw scores for all compounds are shown (Fig. 1B), pooling results across four separate experimental batches in each case. Notable differences were observed in the distribution of compounds inducing resistance (Fig. 1B). The distribution of viability scores for PQ was bimodal, with at least 10% of the tested agents promoting PQ resistance at a level 10-fold above the median value of the remainder of the wells (Fig. 1B, top, red arrow). In this regard, a prior *C. elegans* RNA interference (RNAi) screen for genes regulating PQ resistance showed a similar hit rate as our small molecule screen (*14*). Thus, this relatively high hit rate may reflect multiple pathways deployed by cells to guard against oxidative insult. In contrast,

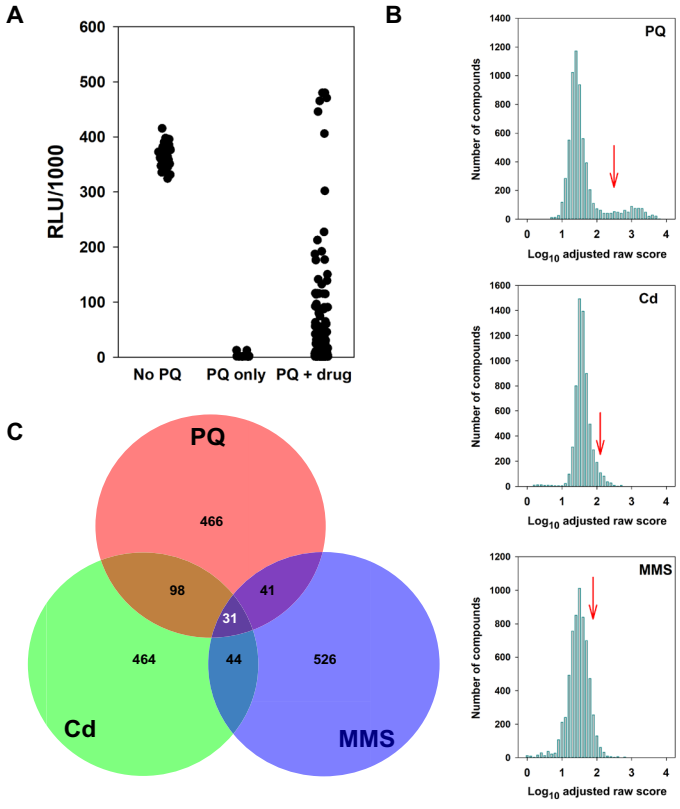

Fig. 1. Primary screen for protection of mouse cells from PQ lethality. (**A**) Example of a single experiment screening 640 compounds. No PQ wells ($n = 32$) received neither PQ nor rescue agent, showing maximum cell viability. PQ-only wells ($n = 32$) show low viability in wells receiving only PQ. PQ + drug ($N = 640$) received PQ plus a test agent. Each symbol designates a different well. RLU, relative light units. (**B**) Histograms for tested agents ($n = 6351$), showing number of tested compounds providing specific degrees of cellular protection for PQ, Cd, and MMS. Scores have been normalized by adjustment for plate-to-plate variation in median cell viability and are expressed on a $\log_{10}$ scale. See Methods for details. Red arrows designate the 90th percentile for each distribution. (**C**) Proportional Venn diagram showing overlap among compounds in the top 10% for induction of PQ, Cd, and MMS resistance in primary screening. Figure generated using http://biovenn.nl/venndiagram.tk/create.php.

the histogram for protection against Cd lethality was asymmetric, but not bimodal, with a tail of compounds yielding cell viability scores above the negative control values or the median of the set of tested compounds (Fig. 1B, middle). In contrast to the other two stressors, few small molecules induced robust protection against MMS in MTFs under these screening conditions (Fig. 1B, bottom).

Compounds that lead to protection against two or more forms of stress (i.e., multiplex stress resistance) may be of particular interest from the standpoint of aging biology. Longevity mutations in *C. elegans* often confer resistance to multiple stressors (*13*), and MTFs from long-lived mice, such as the Snell, Ames, and GHRKO (Growth hormone receptor knockout) strains, are also resistant to multiple stresses (*9*). To test whether drugs that confer resistance to PQ tend also to impart resistance to Cd and/or MMS, we arbitrarily defined each tested agent as protective for the stress if it produced a cell viability score in the upper 10% of the corresponding distribution (Fig. 1C). Of the 636 compounds in the highest 10% for PQ protection, 129 were also in the highest 10% for Cd protection, significantly higher than the 10% expected by chance ($P < 10^{-6}$,

permutation testing). There was no statistically significant enrichment among the top 10% of compounds between PQ and MMS or Cd and MMS. However, among 6351 compounds tested in the primary screen, 31 (0.49%) conferred at least partial protection against PQ, Cd, and MMS, much more commonly than expected by chance ($P < 10^{-6}$, permutation testing). In summary, most of the compounds that imparted resistance to a stressor in primary screening induced resistance to a single agent only, but multiplex stress resistance occurred more frequently than expected by chance for PQ and Cd, and for all three stressors.

To assess the structural diversity of all screened compounds, we performed multidimensional scaling (MDS). The distance matrix required for MDS was generated by all-against-all similarity comparisons using atom pairs as structural descriptors and the Tanimoto coefficient as similarity metric (fig. S1E). The active compounds in the top 10% for all three forms of stress, i.e., PQ, MMS, and Cd in primary screening, are highlighted in red. This analysis emphasizes that compounds that promote multiplex stress resistance are chemically very diverse and do not closely cluster from a structural perspective.

Replication and dose-response experiments

We selected 75 compounds from the primary screen results for further study, either because they provided exceptionally strong protection against PQ or because they were in the top 10% for PQ protection and also provided protection, in the top 10%, for either Cd, MMS, or both (table S2). Some agents which met these criteria were omitted from secondary dose-response (DR) screening because they were not available in pure form in adequate amounts and/or at reasonable cost. We purchased fresh powders of the chemicals that had been tested in primary screening in the HTS test libraries and evaluated them over a range of doses (0.3 to 32 μM) for protection against each of the three stress agents. We classified an agent as protective for PQ stress if, in DR testing, at least one dose promoted a luminescence of ≥100 RLU/1000. For comparison, wells without test agents had luminescence of 10 RLU/1000, and wells with no PQ added had a value of 820 RLU/1000. Thus, categorization as a protective agent required a value 10-fold above the mean negative control. Similar criteria were used to classify the test compounds with respect to protection against Cd or MMS toxicity. This classification was more stringent than that used in the primary screen. Eight of the compounds analyzed in this manner failed DR testing for technical reasons and were not further considered. Among the 67 chemicals for which we successfully obtained DR curves, 52 (78%) were protective against PQ. Among these, 8 also provided protection against both Cd and MMS, 7 provided protection against Cd but not MMS, 10 protected against MMS but not Cd, and the remaining 16 protected against PQ stress alone. Eleven compounds provided protection against PQ but failed testing for the other two stressors for technical reasons. Several agents showed a distinct profile of protection in the primary screen versus DR testing. These discrepancies likely reflect the additional data obtained from DR testing, as well as impurities and/or degradation of the samples in libraries used for primary screening.

The DR data for these 67 agents were used to calculate two parameters for each compound: Max, the highest level of protection produced at any dose, and ED_{50} (median effective dose), the lowest concentration that yielded protection at least as high as Max/2. In addition, a drug was classified as toxic if, at the highest tested dose (32 μM), cell viability was less than Max/2. Rescue agents showed diverse patterns in DR testing; representative DR curves are shown (Fig. 2A). For example, dihydrorotenone provided protection at all tested doses. In contrast, supercinnamaldehyde provided substantial protection against PQ at low doses but was toxic at doses ≥16 μM. Compounds MG 624 and 3230 to 2939 showed sigmoidal DR curves. ED_{50} and Max values for each of the tested agents for protection from PQ toxicity are shown (Fig. 2B). Compounds with Max < 100 RLU/1000

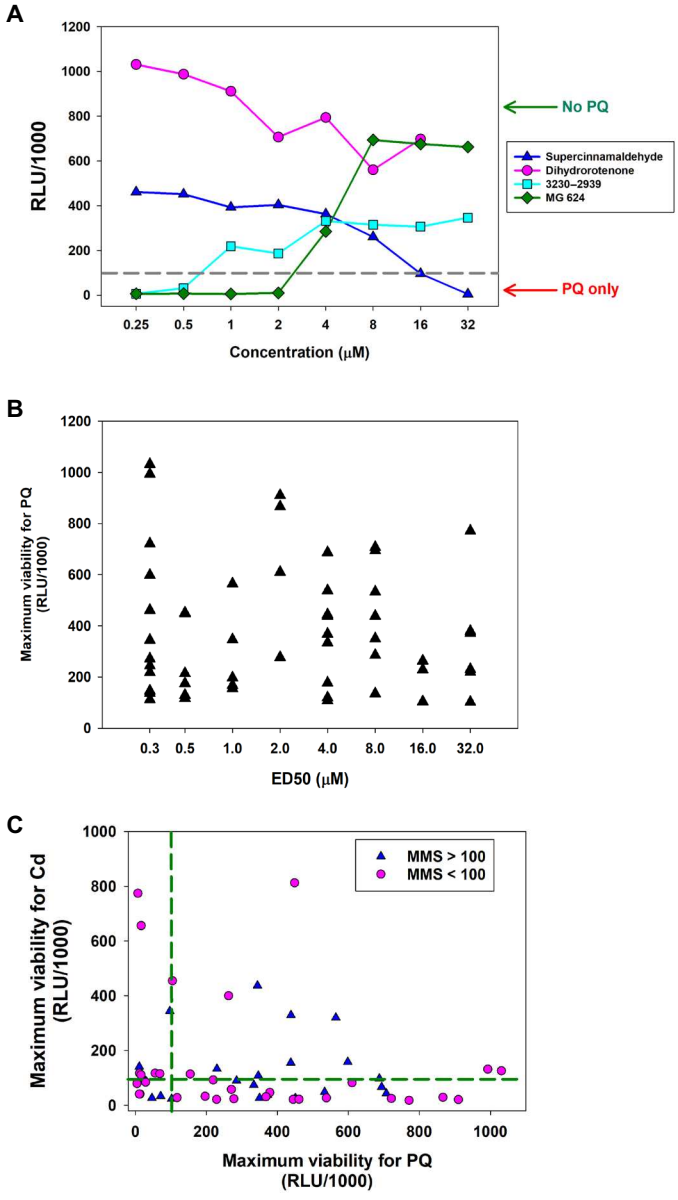

Fig. 2. DR curves for selected small molecules. (**A**) Representative DR curves, for concentrations from 32 to 0.25 μM (*X* axis). Green arrow designates mean score (from four daily batches) for wells with neither PQ nor protective agent added, and red arrow designates mean score for wells that received PQ alone. Gray dashed line shows a viability score of 100, used as an arbitrary criterion for categorizing an agent as protective. (**B**) Scatterplot for ED_{50} versus Max viability score for PQ protection; each symbol represents a different rescue agent. (**C**) Scatterplot showing Max score for PQ protection versus Max protection for Cd stress. Blue triangles indicate rescue agents for which Max > 100 in the MMS protection dose testing. Green dashed lines indicate arbitrary thresholds at Max = 100 for PQ and Cd protection scores.

were considered nonprotective (ED_{50} > 32 μM). Eighteen of the 67 small molecules tested were quite potent, with ED_{50} values of ≤0.5 μM. The maximum level of protection did not correlate with ED_{50} in this set of tested agents.

Max and ED_{50} values for PQ, Cd, and MMS for each of the 67 compounds with DR data are provided (table S2). An overview of relationships between Max values for PQ and Max values for Cd for each drug is shown (Fig. 2C). Many agents provided robust protection against PQ but not Cd, and a few protected against Cd but not PQ, despite having been initially selected based on a screen for PQ resistance at the single 16 μM dose in primary screening. Drugs that yielded protection against MMS are indicated (Fig. 2C, blue triangles). Seven compounds conveyed Max > 100 RLU/1000 for all three stress agents. However, there was not a strong correlation between Max values for PQ and Cd nor a strong tendency for agents that protect against PQ and Cd to protect cells against MMS as well.

Relationship between induction of MTF stress resistance by small molecules and lifespan extension in *Drosophila* or *C. elegans*

Because enhanced stress resistance is a conserved feature of extended longevity, we tested whether compounds identified in HTS in MTFs would extend lifespan in *Drosophila melanogaster* and *C. elegans*, invertebrate models often used for studies of aging and lifespan. We fed both *C. elegans* and *D. melanogaster* with selected small molecules over the entire lifespan and assayed survivorship (table S3) to test the hypothesis that compounds that improved cellular survival in response to stress would be more likely to induce invertebrate lifespan extension compared to compounds with little or no effect on MTF survival.

In flies, drugs were tested at 20 μM in females and at 200 μM in males. These doses were selected on the basis of a prior study in which rapamycin treatment of flies extended lifespan (*16*). A compound was scored as positive if it increased lifespan in either sex compared to dimethyl sulfoxide (DMSO) control, by log-rank test at $P = 0.05$ or better. Among the 70 unique compounds that significantly increased MTF stress resistance that were tested in flies, 12 significantly increased fly lifespan in either or both sexes (17.1% of the total compounds tested) (table S3). However, 16 of 54 negative control compounds tested (i.e., those that did not induce MTF stress resistance) were also able to significantly increase fly lifespan (29.6% of the total compounds tested; $P = 0.07$ for hits versus negative controls). No tested agent increased median lifespan by more than 20%.

In *C. elegans*, compounds were tested in hermaphrodite worms at two concentrations, 10 and 100 μM (table S3). The concentrations were selected on the basis of several papers in which drug treatments were shown to extend *C. elegans* lifespan (*3*, *17*, *18*). A compound was scored as positive if it significantly increased lifespan by log-rank test at $P = 0.05$ or better, at one or both doses. Fifteen of 70 (21.4%) compounds that increased MTF stress resistance extended worm lifespan, as did 6 of 54 (11.1%) negative control compounds ($P = 0.15$). If we consider compounds that extended lifespan in either or both invertebrate organisms, 26 of 70 hit compounds extended lifespan (37.0%), as did 20 of 54 negative control compounds ($P = 0.99$). Thus, in this relatively small dataset, a set of agents selected for their ability to protect MTFs from stress were not enriched in compounds that extend fly or worm lifespan. Reproducibility between the model organisms was poor. Overall, 89 drugs were tested in common between flies and worms. Among these, only five increased lifespan in both female flies and in worms. No drugs showed concordant lifespan results between worms and both sexes of flies or between worms and male flies. Fourteen drugs showed discordant lifespan results between worms and both sexes of flies.

To extend this analysis, we took advantage of the fact that one of the libraries screened for lifespan effects in our primary MTF screen, the LOPAC collection, had previously been assayed for effects on worm lifespan by Ye *et al.* (*6*). Among the 1280 compounds in the LOPAC library, we were able to match 827 between our HTS and the data tabulated by Ye *et al.* A caveat to this analysis is that, since the latter publication did not provide compound structure information, matching entries among the two datasets used chemical names and formatting differences may have introduced errors. We considered "hits" from the HTS to be those that were in the top 10% for PQ, MMS, or Cd; this amounted to 207 of 827 or 25% of the total (table S4). We considered the "hits" from the Ye paper to be compounds in the top 10% of positive change in lifespan, representing a 15% lifespan increase or better. Among the 207 hits from our HTS, 34 were also in the top 10% for lifespan increase (16.4%). However, among the 620 compounds in the bottom 90% for all three stressors in the cell screen, only 40 were in the top 10% for increased worm lifespan in the results of Ye and colleagues (6.5%), indicating a highly significant association between induction of cellular stress resistance and *C. elegans* longevity ($P < 0.0001$, Fisher's exact test). By contrast, if we selected 200 random compounds, none of which were hits in our HTS, we find that 16 (8%) were in the top 10% of increased lifespan in the study by Ye *et al.* Among the remaining 627 compounds not in the randomly selected group, 58 were in the top 10% of increased lifespan (9.2%), $P = 0.67$ (nonsignificant) by Fisher's exact test. In summary, although our own small-scale analysis did not identify a significant relationship between small-molecule induction MTF stress resistance and lifespan extension in *C. elegans*, a much better-powered comparison with a published *C. elegans* screen did suggest such a relationship.

In our *C. elegans* lifespan studies, among the agents scoring positive for extension of lifespan at both 10 and 100 mM, in two separate trials, was the antibiotic tetracycline (Fig. 3A). This is consistent with prior results showing that interventions that selectively impair mitochondrial protein synthesis can increase worm lifespan (*19*). Likewise, the mitochondrial poison dihydrorotenone increased worm lifespan at two doses (Fig. 3B), consistent with the known ability of mitochondrial defects present at specific developmental stages to extend longevity in this organism (*20*). Both of these agents robustly promoted PQ resistance in MTFs (table S1), suggesting that these drugs may exert conserved effects in worms and mammalian cells, potentially via impairment of mitochondrial function.

Associating screening hits with known drugs, target proteins, and pathways

We used fragment-based structural similarity searches combined with the Tanimoto coefficient to identify nearest structural neighbors in DrugBank (*21*) for the 4920 unique agents for which we had acquired cell stress resistance data in primary screening (*22*, *23*). DrugBank was chosen as the reference database for this purpose because it represents one of the most comprehensive and best curated collections of drugs available in the public domain. This allowed us to obtain detailed functional annotations from DrugBank for many of our screened compounds, including therapeutic usage and target proteins (*24*, *25*). Among the compounds used for our primary

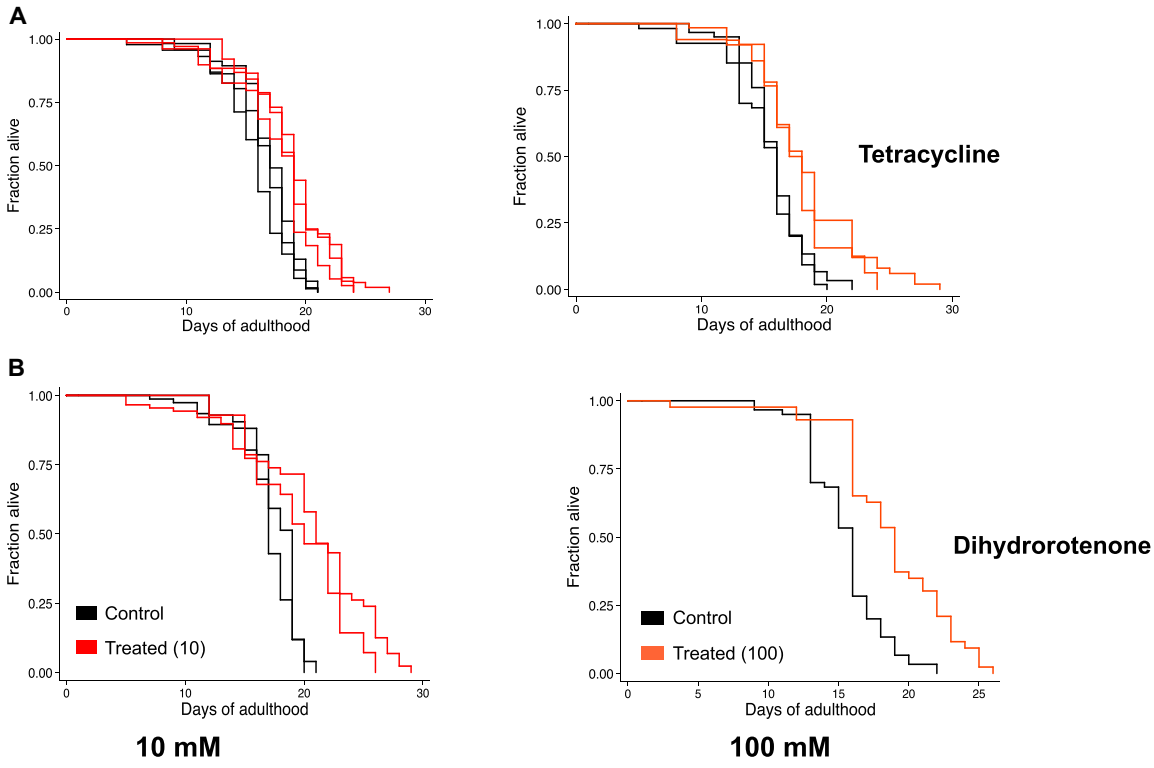

Fig. 3. Tetracycline and dihydrorotenone increase lifespan in C. *elegans*. Representative Kaplan-Meier survival curves of *C. elegans* treated with tetracycline (**A**) or dihydrorotenone (**B**). Experimental replicates are shown as multiple lines.

screens, 1935 (39%) were represented in DrugBank based on a Tanimoto coefficient of ≥0.9. Nearly all DrugBank compounds for our screening hits were annotated with at least one target protein. The results of this in silico analysis, including target protein annotations, are presented in tables S5 and S6.

We then performed functional enrichment analysis (FEA) on the groups of compounds identified as hits in the PQ and Cd screens, as well as both of them (PQ and Cd). As functional annotations systems we included here gene ontologies (GO), disease ontologies (DO), or Kyoto Encyclopedia of Genes and Genomes (KEGG) pathways (*26*–*29*). Two complementary enrichment methods were used for this: target set enrichment analysis (TSEA) and drug set enrichment analysis (DSEA). For TSEA, the compound sets were converted into target protein sets based on the drug-target annotations obtained from DrugBank in the previous step. The corresponding gene sets for these target sets were used as test samples to perform TSEA with the hypergeometric distribution. Because several compounds in a test set may bind to the same target, the test sets can contain duplicate entries. This corresponding frequency information will be lost in traditional enrichment tests, because they assume uniqueness in their test sets, which is undesirable for FEA of compounds. To overcome this limitation, we also performed DSEA on the active compound sets themselves (here test sets) against a database containing compound-to-functional category mappings. The latter was generated by substituting the targets in the former by the compounds they bind. The main advantage of DSEA is that it maintains functional enrichment information in situations when several compounds bind to the same target, because there are usually no duplicates in compound test sets. The enrichment results for TSEA and DSEA are available in tables S7 and S8, respectively.

As expected, the DSEA results are not identical to the TSEA results but share several top-ranking functional categories. For brevity and consistency, the following evaluation of the FEA will focus on the TSEA results. The most highly enriched functional categories found in the TSEA for the PQ (fig. S2A) and Cd (fig. S2B) screens were very similar with respect to both their compositions and their rankings by enrichment *P* values. The agreement among two relatively distinct methods demonstrates the robustness of the obtained rankings of functional categories. The most common GO term and KEGG pathway annotations among the top-scoring categories are related to receptor and transporter functions and signaling pathways. Another interesting finding is that the two most highly enriched DO terms in both the PQ and Cd screen (table S7) are associated with age-related diseases, such as congestive heart failure (DOID:6000; adjusted $P = 2.08 \times 10^{-6}$) and heart disease (DOID:114, adjusted $P = 2.35 \times 10^{-6}$). On the basis of the pharmacodynamics annotations from DrugBank (table S5), the test sets used for the enrichment analyses of both screens include FDA-approved drugs that are used to treat cardiovascular conditions.

Transcriptomic analysis reveals that AEG3482 and cardamonin induce Nrf2 target genes

To gain additional mechanistic insight into how compounds identified by HTS confer stress resistance, we performed RNA sequencing (RNA-seq) analysis (*30*–*32*) on MTFs treated with eight compounds: AEG 3482, antimycin A, berberine HCl, cardamonin, clofilium tosylate, dihydrorotenone, diphenyleneiondonium HCl, and podofilox. These compounds were selected because of their robust induction of stress resistance, modest cost, and biological interest. Principal components analysis (PCA) of the RNA-seq data plotted on the first

two principal components showed that five compounds clustered together with DMSO in PC1 (principal component 1) and, to a lesser extent, in PC2 (principal component 2) (Fig. 4A). Treatments with these compounds did not elicit a transcriptional response much different from DMSO. In contrast, three other compounds (AEG 3482, cardamonin, and podofilox) induced a much greater degree of transcriptomic heterogeneity (Fig. 4A) and differed from one another markedly in PC1.

To identify differentially expressed (DE) genes for each compound compared to the DMSO control, a significance threshold of (false discovery rate) FDR < 0.05 and $\log_2$ fold-change threshold of >1 or ≤1 were imposed. Unsupervised hierarchical clustering analysis (HCA) based on the top 50 genes with greatest variance from the mean revealed that AEG 3482 and cardamonin clustered together, while the other six small molecules tested clustered together with each other and with DMSO control (Fig. 4B). In analysis of a larger group of the 300 most variant genes, this clustering was maintained (fig. S3). Overall, cardomonin and AEG 3482 induced (i) a larger number of DE transcripts and (ii) changes in these transcripts of greater magnitude compared to DMSO control (table S9).

To elucidate potential mechanisms by which these compounds induce stress resistance, we performed functional analysis of DE genes using QIAGEN Ingenuity Pathways Analysis (IPA) and gene set enrichment analysis (GSEA) (*33*). Cellular immune response and cytokine signaling–related terms were identified as significantly affected IPA-defined pathways for all eight compounds; many of the genes involved relate to cytokine signaling and innate immunity (table S10). For AEG 3482 and cardamonin, manual inspection of IPA and GSEA results revealed a strong oxidative stress resistance signature, including Nrf2-mediated oxidative stress response (table S11). This strong Nrf2 antioxidant gene expression signature was not evident for the six other compounds (table S11). The transcription factor nuclear factor erythroid 2–related factor 2 (NFE2L2, also known as Nrf2) is a core mediator of the cellular response to oxidative stress (*34*). In HCA (Fig. 4B), all of the genes most strongly up-regulated by cardamonin and AEG3482 were either well-known Nrf2 targets (*Scl7a11*, *Srxn1*, *Gsta1*, *Hmox1*, *Gsta2*, *Gsta4*, and *Gdf15*) or have Nrf2 promoter binding sites (*Camk1d* and *Ednrb*) (NRF2-20460467-MEF-MOUSE, (*35*)). In *C. elegans*, the Nrf2 homolog, SKN-1, is required for lifespan extension induced by reduced mTOR signaling, as well as multiple other genetic, dietary, and pharmacologic prolongevity interventions (*36*). In mice, although Nrf2 is dispensable for longevity induced by calorie restriction (*37*), a mixture of plant extracts that activates Nrf2 extends lifespan in male mice (*38*). Given these data linking Nrf2 signaling to lifespan, we focused functional studies on Nrf2/SKN-1 as a potential target of AEG 3482 and cardamonin.

IPA revealed several pathways related to Nrf2 oxidative stress induced by AEG 3482 and cardamonin (Fig. 5A). Likewise, GSEA of the RNA-seq data showed that Nrf2 induction and glutathione conjugation, a key transcriptional target pathway of Nrf2, were highly enriched pathways induced by cardamonin (Fig. 5B) and AEG 3482 treatment (fig. S4). Similarly, the high normalized enrichment score calculated by GSEA indicates that genes induced by Nrf2- and Nrf2-related pathways are overrepresented at the top of the ranked list of RNA-seq gene expression changes; thus, cardamonin and AEG 3482 treatment preferentially induces activation of these pathways. Glutathione *S*-transferases neutralize a wide range of electrophilic molecules, including reactive oxygen species (ROS) (*34*). Other antioxidant defense mechanisms regulated by Nrf2 include synthesis and regeneration of cellular reducing agents—i.e., glutathione (reduced form) (GSH)—expression of genes in the antioxidant thioredoxin (TXN) system and regulation of heme metabolism (*39*).

Under basal conditions, Nrf2 is actively polyubiquitinated and degraded by the Keap1/Cul3 complex but is stabilized in response to various insults, in particular, oxidative or xenobiotic stress (*34*). In RNA-seq analysis, *NFE2L2* mRNA was not induced by any of the compounds when compared to the DMSO control. From the RNA-seq analysis, we also extracted the best-characterized genes representative of an Nrf2 response signature (Fig. 5C) (*34*, *39*, *40*). Expression of genes involved in GSH synthesis, utilization, and regeneration were all markedly increased in response to AEG 3482 and cardamonin. In addition to GSH-related genes, AEG 3482 and cardamonin also induced expression of genes in the TXN pathway, which reduces oxidized protein thiols (Fig. 5C). These changes did not occur in response to the six other compounds tested (fig. S5). Oxidized TXN is reduced to a functional form by TXN reductase (*Txnrd1*) (*40*). Transcripts encoding heme oxygenase (*Hmox1*) and *Ftl1*, important for the proper catalytic degradation of heme and Fe^{2+} storage, were also up-regulated by AEG 3482 and cardamonin (Fig. 5C). Improper degradation of heme can result in generation of free Fe^{2+}, which can then catalyze conversion of H_2O_2 to damaging hydroxide radical (*39*). To confirm that changes observed by RNA-seq were reflected at the protein level, we performed immunoblot analysis for GCLC (Glutamate-Cysteine Ligase Catalytic Subunit) and GCLM (Glutamate-Cysteine Ligase Modifier Subunit) (subunits of glutamate cysteine ligase, involved in the glutathione synthesis pathway Fig. 5D), and Hmox1 at 48 hours after compound treatment. Consistent with mRNA expression data, AEG 3482 and cardamonin, but not podofilox, increased protein expression of these Nrf2 targets (Fig. 5, D and E).

Cardamonin and AEG 3482 activate SKN-1 signaling in *C. elegans* to promote oxidative stress resistance

We tested whether the HTS hits characterized by RNA-seq also promoted stress resistance in worms (Fig. 6A). Among the eight compounds tested, five, including AEG 3482 ($P < 5 \times 10^{-13}$, log-rank test) and cardamonin ($P < 8 \times 10^{-10}$, log-rank test), enhanced worm survival in response to PQ challenge. We performed assays to test whether cardamonin and AEG 3482 activated SKN-1/Nrf2 signaling and PQ resistance in the worm. We used a worm strain containing a *gst-4p::gfp* reporter, in which GFP expression is driven by SKN-1 activity. We found that AEG 3482 and cardamonin, as well as PQ itself, induced highly significant induction of GFP fluorescence (Fig. 6B and fig. S6). As a negative control, podophyllotoxin, which did not activate Nrf2 signaling according to RNA-seq analysis, did not induce GFP expression in the SKN-1 reporter strain. Lastly, to test whether cardamonin and AEG 3482 acted through SKN-1 to promote oxidative stress resistance in worms, we repeated the PQ challenge in a *skn-1* mutant background (Fig. 6C). Cardamonin and AEG 3482 both induced a partial, highly significant rescue of PQ-induced lethality in wild-type worms ($P < 2 \times 10^{-10}$ and $P < 1 \times 10^{-13}$, respectively, by log-rank test). However, neither compound showed significant rescue activity of PQ toxicity in *skn-1* mutant worms ($P < 0.4$ and $P < 0.09$ for cardamonin and AEG 3482 by log-rank, respectively, both nonsignificant). By Cox regression analysis, the *P* values for the interaction terms between drug and genotype were 9.3×10^{-7} (AEG 3482) and 7.3×10^{-6} (cardamonin), respectively, both highly significant. Together, our findings demonstrate

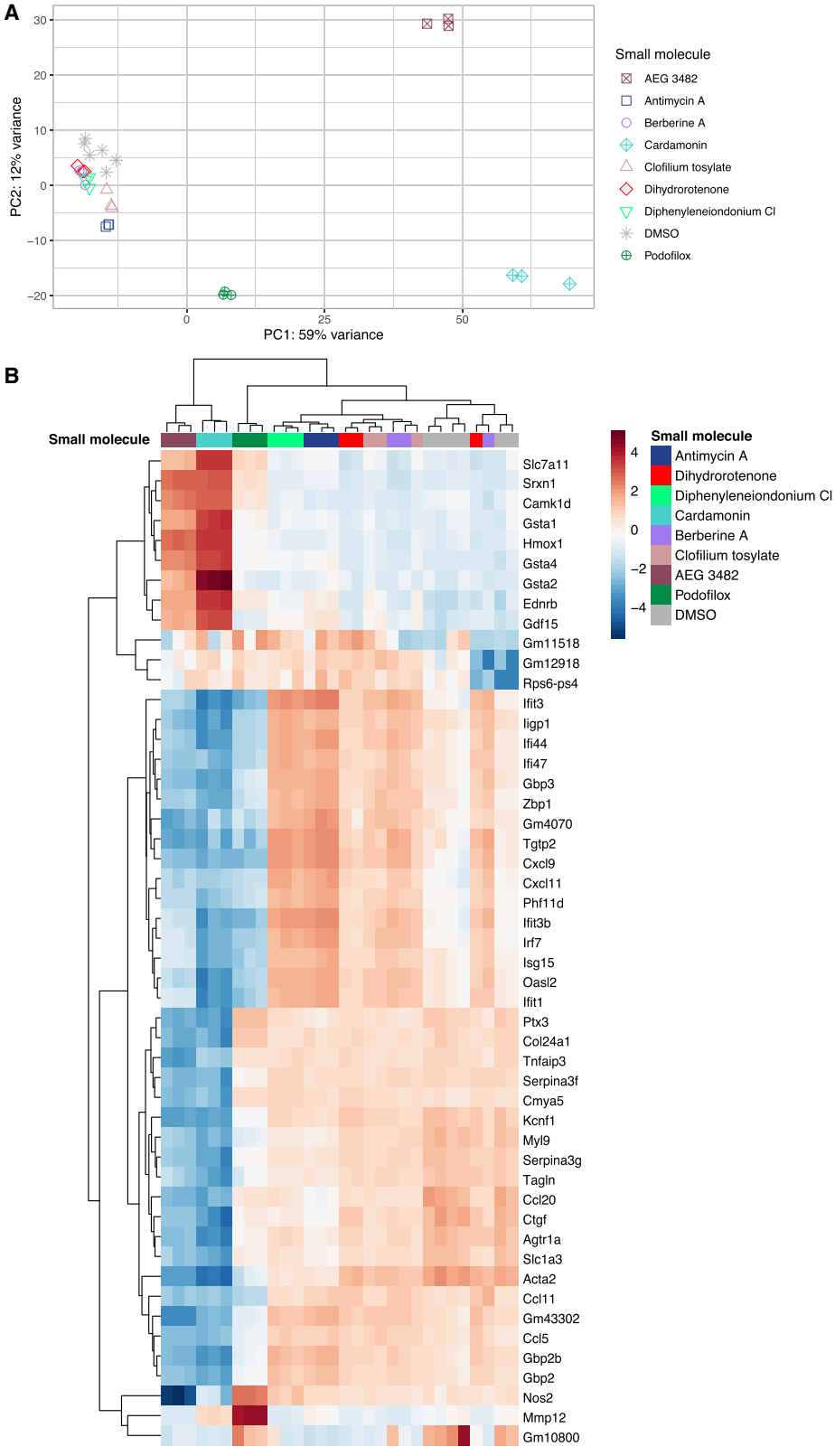

Fig. 4. Transcriptomic analysis of eight rescue compounds. (**A**) PCA for all RNA-seq samples. (**B**) Dendrogram with unsupervised hierarchal clustering of the top 50 genes with greatest variance from the mean. Expression across each gene (row) has been scaled such that the mean expression is zero (pale yellow). Red indicates high expression in comparison to the mean. Blue indicates low expression in comparison to the mean. Lighter shades represent intermediate levels of expression. PC1, principal component 1.

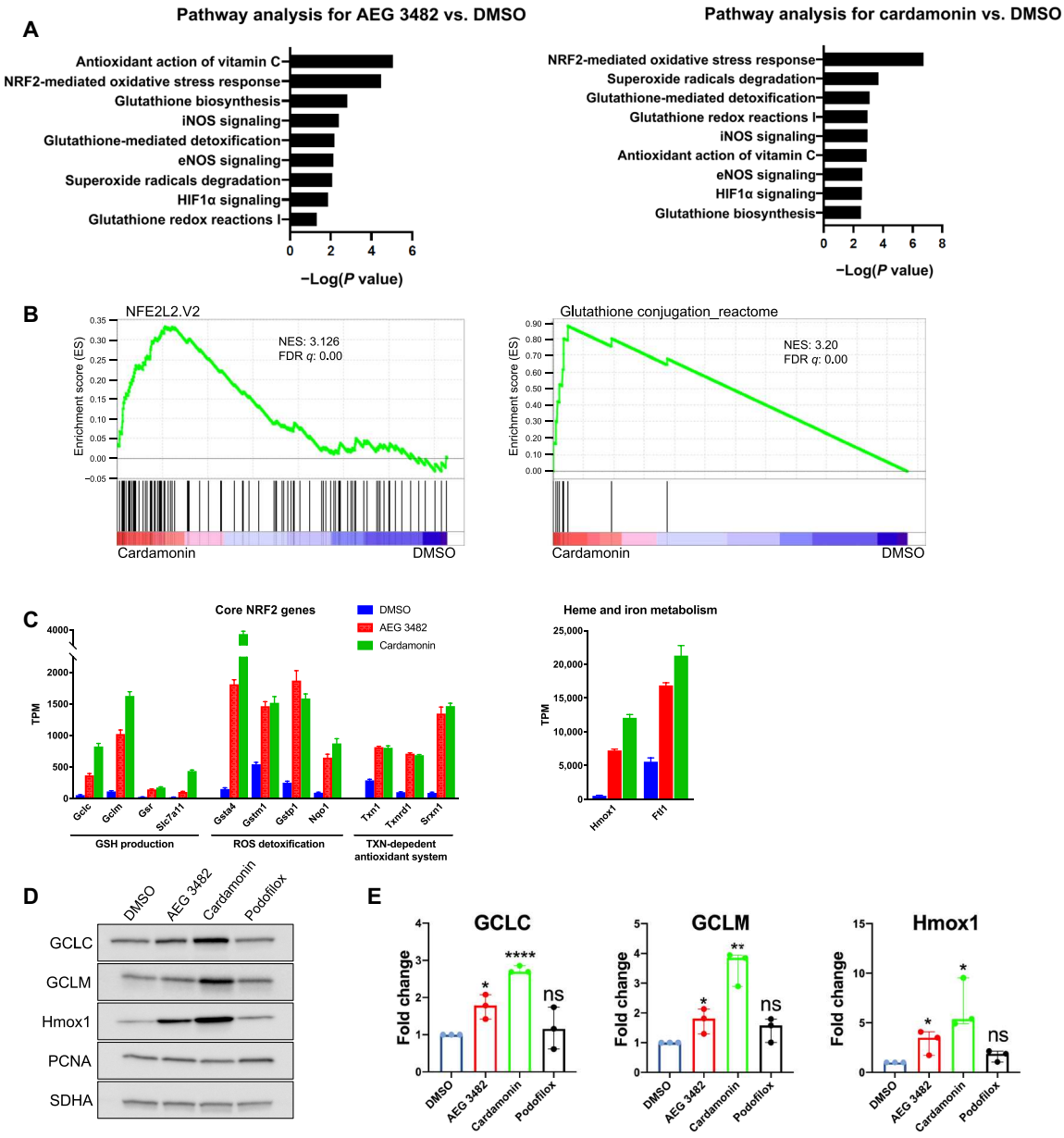

Fig. 5. Nrf2 antioxidant signature in response to AEG 3482 or cardamonin treatment. (**A**) Pathways related to oxidative stress response from IPA for DE genes induced by AEG 3482 and cardominin. *P* values represented in negative log form; all pathways are significant at $P < 0.05$. eNOS, endothelial nitric oxide synthase; iNOS, inducible nitric oxide synthase. (**B**) GSEA for cardamonin for pathways indicated. NES, normalized enrichment score. (**C**) Transcripts in key pathways induced by Nrf2 are significantly elevated by AEG 3482 and cardamonin treatment. All FDRs for comparison to DMSO are $q < 5 \times 10^{-6}$. TPM, transcripts per million. (**D**) Immunoblot analysis of Nrf2 targets after treatment with indicated compounds for 48 hours. PCNA and SDHA serve as loading controls. (**E**) Immunoblot in (D) was performed three times using independent biological samples. Band intensities were quantified by ImageJ and then normalized to control loading band (SDHA or PCNA). Mean and SEM are designated. Each treatment was compared to DMSO via two-tailed unpaired *t* test. $^*P < 0.05$, $^{**}P < 0.01$, and $^{****}P < 0.0001$. ns, not significant.

that cardamonin and AEG 3482 activate Nrf2/SKN-1 signaling in an evolutionarily conserved manner and that these small molecules act through SKN-1/Nrf2 in *C. elegans* to promote PQ resistance.

Proteomic analysis reveals widespread changes in cellular signaling pathways induced by hit compounds

Besides AEG 3482 and cardamonin, the other six compounds did not induce an Nrf2 transcriptional signature, suggesting that they function through other pathways to promote cellular stress resistance. To identify such candidate pathways, we performed reverse phase protein array (RPPA) analysis on the same eight compounds tested in RNA-seq. RPPA is a high-throughput antibody-based approach that permits simultaneous assessment of levels of hundreds of proteins and phosphoproteins (*41*). In this analysis, we found that the eight compounds induced apparent changes in multiple signaling pathways relevant for cellular stress resistance, survival, and longevity, including AMPK (5' AMP-activated protein kinase), Akt, mTOR, and others (fig. S7), potentially rationalizing the effects of these small

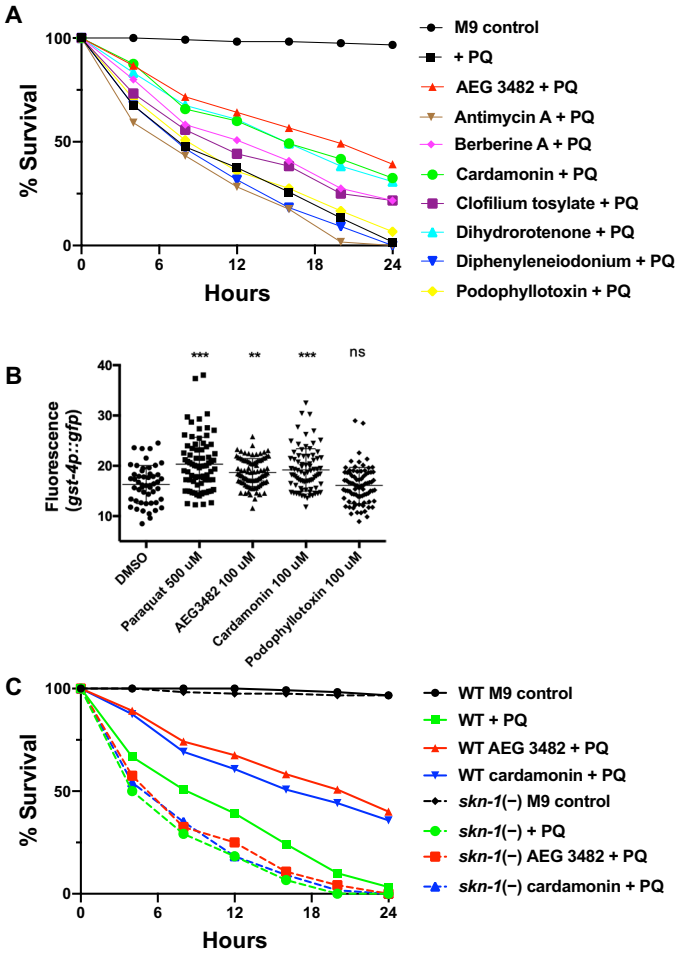

Fig. 6. Cardamonin and AEG 3482 promote SKN-1–dependent PQ resistance in *C. elegans*. (**A**) Increased PQ resistance conferred to *C. elegans* by cardamonin and AEG 3482 and three other compounds analyzed by RNA-seq. Log-rank *P* values versus PQ alone are as follows: 5×10^{-13} AEG 3482, 8×10^{-10} cardamonin, 6×10^{-9} dihydrorotenone, 7×10^{-5} berberine, 7×10^{-4} clofilium tosylate, 0.4 podophyllotoxin, 0.4 diphenyleneiodonium, and 0.01 antimycin A. (**B**) PQ, cardamonin, and AEG 3482, but not podophyllotoxin, induce the expression of a *gst-4p::gfp* reporter. Each point designates fluorescence in an individual worm treated as indicated. DMSO was compared to other treatments by one-way analysis of variance (ANOVA). See fig. S6 for two additional experimental replicates. ***$P < 0.001$ and **$P < 0.01$. (**C**) PQ resistance induced by cardamonin and AEG 3482 requires intact SKN-1 function. Log-rank *P* values are as follows: WT M9 v. WT + PQ 2×10^{-16}; *skn-1*(−) M9 v. *skn-1*(−) + PQ 2×10^{-16}; WT + PQ v. WT AEG 3842 + PQ 1×10^{-13}; WT + PQ v. WT cardamonin + PQ 2×10^{-10}; *skn-1*(−) + PQ v. *skn-1*(−) AEG 3482 + PQ 0.09; *skn-1*(−) + PQ v. *skn-1*(−) cardamonin + PQ 0.4.

molecules on stress resistance. Future studies will be required to elucidate the impact of these molecular changes on cellular stress resistance.

DISCUSSION

The unbiased identification of compounds that can enhance mammalian health- and lifespan represents a major challenge. Resistance to multiple forms of environmental insult is a common feature of longevity, among different species, in invertebrate aging models, and in genetically engineered strains of mice (*9*). In this work, we performed HTS to identify small molecules that promote stress resistance in mouse fibroblasts and identified compounds promoting survival in response to PQ, Cd, and MMS, as well as multiplex stress resistance. The ability of small molecules to increase fibroblast stress resistance was not strongly correlated with extension of worm or fly lifespan in our own smaller-scale experiments, but there was a strong correlation in a larger, previously published *C. elegans* dataset (*6*). Transcriptomic analysis and *C. elegans* genetic studies identified Nrf2/SKN-1 signaling as the functionally relevant pathway involved in stress resistance provoked by two hits, cardamonin and AEG 3482. Some of the compounds identified in our studies—particularly those that induce multiplex stress resistance—may merit further mechanistic studies in cells and perhaps subsequent evaluation in whole animals.

Some of the compounds identified as hits in our HTS have previously been investigated for their potential health benefits. For example, epigallocatechin-3-monogallate— which promotes PQ and MMS resistance in our DR studies—is a polyphenol present in green tea, claimed to have beneficial properties against cancer and cardiovascular disease (*42*). Carvedilol, found to promote PQ and Cd resistance in our DR studies, is a β-adrenergic blocker with anti-α1 activity, clinically useful in patients with heart failure. It is possible that some of the cardioprotective effects of this agent occur in part through promotion of cellular stress resistance in cardiomyocytes, although we have not directly assessed the effects of carvedilol on this cell type. Likewise, cardamonin is a spice-derived nutraceutical with anti-neoplastic and anti-inflammatory properties, which may involve modulation of the activity of STAT3 (Signal transducer and activator of transcription 3) and other transcription factors (*43*).

It is notable that several compounds that induce PQ resistance—antimycin A, dihydrorotenone, rotenone, tetracycline, chloramphenicol, and rifampicin (table S1)—are known mitochondrial toxins. The mitochondrion represents an important site for PQ-mediated ROS production (*44*); hence, interference with mitochondrial function by these small molecules may reduce ROS production and subsequent cellular toxicity induced by PQ. Alternatively or in addition, this phenomenon may reflect hormesis (*45*), i.e., the cellular response to mitochondrial dysfunction induced by these rescue agents may prime the cell to more effectively respond to PQ toxicity.

Our approach has several potential limitations. Cellular stress resistance is a complex phenotype influenced by numerous signaling pathways, which may have led to the unexpectedly high initial hit rate (approximately 10% against PQ in primary screening), and the chemical diversity and large number of potential targets of our protective compounds. Note that an RNAi screen in *C. elegans* for genes regulating PQ resistance showed a similar hit rate to our small-molecule screen (*14*). Our primary screening was carried out at a single concentration of rescue compound (16 μM), thus potentially missing chemicals that may be effective at lower or higher doses but ineffective or even toxic at the particular dose used in the screen. Highlighting these limitations, among drugs found to extend lifespan reproducibly in one or both sexes of mice in ITP studies (https://nia.nih.gov/research/dab/interventions-testing-program-itp), the three that we also tested (rapamycin, acarbose, and canagliflozin) did not increase resistance to PQ, MMS, or Cd, nor did dapagliflozin, a drug closely related to canagliflozin. In this regard, it is important to note that many compounds that extend mouse lifespan would be unlikely to yield a positive result when tested in our system. Acarbose, for example, is thought to modulate blood glucose by affecting starch digestion in the gastrointestinal tract, for which there is no in vitro cellular analog. Similarly, canagliflozin alters renal and intestinal glucose retention, a process without in vitro parallels, and 17α-estradiol

may require conversion to another steroid before acting on targets in the central nervous system. Compounds that increase stress resistance of specific cell types, such as neurons or hepatocytes, might be missed by our screening strategy, because we have focused on only a single cell type, MTFs. Similarly, our strategy will not identify compounds that require metabolic transformation in vivo, e.g., in the liver, for biological activity nor will compounds that affect interorgan signaling to extend longevity.

Compounds that increased resistance of mouse fibroblasts to multiple forms of stress were enriched, compared to the overall set of tested agents, for the ability to promote *C. elegans* lifespan in a prior large-scale screen (*6*). However, this correlation was fairly weak, as no such relationship existed in our smaller-scale *C. elegans* and *Drosophila* studies, and moreover, there was no significant overlap in drugs that extended lifespan in common between these organisms. There are many caveats to the invertebrate experiments. For example, we do not know whether worms and flies consume food similarly on all compounds administered to them, nor do we know the optimal dose of each compound in the invertebrate models, nor how well the compounds may penetrate the cuticle. Overall, the data suggest that, as a general matter, it is not straightforward to identify compounds that increase invertebrate lifespan by selecting drugs that increase stress resistance of cultured mammalian cells, unless a large number of compounds are screened. Nevertheless, PQ resistance has successfully been used as a surrogate phenotype in an RNAi screen to identify longevity mutants in *C. elegans* (*14*). Moreover, in worms, many mutants with increased lifespan also show elevated stress resistance (*13*). Notable among these is the *daf*-2 mutant, which displays greatly extended longevity and multiplex stress resistance: enhanced survival in response to oxidative, heavy metal, heat, and infectious insults. These findings emphasize not only the evolutionarily conserved nature of the link between oxidative stress resistance and lifespan, but also the challenges in screening invertebrate organisms for lifespan-extending compounds.

Among the eight compounds analyzed via RNA-seq, two—cardamonin and AEG 3482—strongly activated Nrf2/SKN-1 signaling and antioxidant defenses in an evolutionarily conserved manner, an activity that was required in worms for promotion of PQ resistance. Nrf2 regulates expression of numerous cytoprotective genes via binding to promoter antioxidant response elements in response to oxidative or xenobiotic insult. Nrf2 inducers are under development for a variety of inflammatory, metabolic, degenerative, and neoplastic diseases. The induction of Nrf2 signaling by cardamonin that we observe is consistent with prior reports in the literature (*46*). In this regard, Nrf2 levels and target gene expression are elevated in skin fibroblasts derived from long-lived Snell dwarf mice, likely contributing to the multiplex stress resistance observed in these cells (*47*). Although Nrf2 is dispensable for longevity induced by calorie restriction in mice (*37*), a mixture of botanical extracts that induces Nrf2 extends median lifespan in male mice (*38*). These observations are consistent with the notion that some of the hits identified using this HTS approach may exert beneficial longevity effects in mammals.

AEG 3482 was originally identified by its ability to suppress death of cultured neurons following growth factor withdrawal (*48*). It is thought to act via binding to HSP90 (Heat shock protein 90) to induce HSF1 (Heat shock factor 1) activity, increase HSP70 expression, and suppress c-Jun N-terminal kinase signaling. In MTFs, using our experimental conditions, AEG 3482 provoked only a weak "cellular response to heat" signature by GSEA (fig. S8); the related signature, "heat shock protein response", was nonsignificantly induced. Extensive cross-talk between HSF1 and Nrf2 (nuclear factor erythroid 2–related factor 2) signaling occurs; these transcription factors are known to regulate overlapping sets of genes (*49*). Chemically distinct Nrf2 activators are reported to induce an HSF1 target gene (*50*). Thus, it is possible that HSF1 responses contribute to the stress resistance induced by AEG 3482 and/or cardamonin. The other six small molecules analyzed did not produce a clear Nrf2 or antioxidant gene expression signature. These compounds may promote stress resistance via their effects on cellular inflammatory pathways or by regulating other upstream signaling pathways. Future studies are needed to elucidate their mechanism of action. Moreover, according to our RNA-seq results, both cardamonin and AEG 3482 also affect other cellular pathways besides Nrf2, such as nitric oxide signaling; it will be of interest to explore other pathways affected by these drugs in future studies.

While this study was under revision and subsequent to its deposition at bioRxiv (https://biorxiv.org/content/10.1101/778548v1), Zhang *et al.* (*51*) described the results of a screen in which they identified small molecules that promoted resistance to hydrogen peroxide in human fibroblasts. As in our study, several of their hits appeared to activate Nrf2 signaling, consistent with the known role of this pathway in oxidative stress response. One of their protective compounds was a member of the chalcone class of chemicals, which also includes cardamonin. Among the 32 "core" hits characterized in the study of Zhang *et al.*, nine (28%) were found to extend lifespan in *C. elegans*, a roughly similar fraction as in our study, 15 of 70 (21%). Zhang *et al.* did not assess the effects of a group of control compounds that were not identified as hits in their mammalian cell screen on worm lifespan; hence, the rate of "background" positivity in their study is unclear. Nevertheless, together, our complementary studies highlight the ability of screens for cellular stress resistance to identify biologically active small molecules for downstream analysis.

In summary, we have performed HTS to identify compounds that confer protection against multiple forms of cytotoxic insult to mammalian cells. These hits—particularly the agents that induce resistance to multiple stressors—may prove to be useful tools to probe mechanisms of cellular stress resistance and to test for beneficial effects in rodent models. More broadly, the strategy presented here may represent a workflow for screening larger compound libraries to identify new candidate antiaging molecules with potential health benefits.

MATERIALS AND METHODS

Cell generation

Mouse fibroblast cell lines were established using pooled tail fibroblasts from five male and five female genetically heterogenous UM-HET3 mice, each 8 to 11 weeks old. Cell lines were started from each donor mouse and grown to a minimum of 20 million cells simultaneously. Twenty million cells from each donor mouse were thoroughly mixed, and aliquots of 2×10^6 cells were cryopreserved at passage 2. Cells were thawed as needed and passaged twice after thawing. At the second passage, cells were suspended in high-glucose Dulbecco's modified Eagle's medium (DMEM) without sodium pyruvate and supplemented with 10% fetal bovine serum and penicillin/streptomycin/amphotericin B. Cells were kept in a 37°C, 10% CO_2 and humidified incubator.

Stress resistance assays

On day 1, MTFs were suspended at a concentration of 10,000 cells/25 μl (0.4×10^6 cells/ml) in DMEM plus 0.5% BSA. Cells were then

aliquoted into 384-well plates (Greiner catalog no. 781080) and incubated overnight at 37°C in a 10% humidified CO_2 incubator. On day 2, 0.2 μl of test compounds (plate columns 3 to 22) or DMSO (plate columns 1 to 2 and 23 to 24) were added, for an initial compound concentration of 16 μM and initial DMSO concentration of 0.8%. Plates were then incubated overnight. On day 3, 5 μl of medium alone (columns 1 and 2) or medium plus stress agent (columns 3 to 24) were added to plates. Typical final concentrations of stress agent used in primary screens were 12 mM PQ, 4 μM Cd, and 0.76 mM MMS. In some studies, 15 mM PQ and 12 μM Cd were used in parallel with the more standard stress conditions. On day 4, 5 μl of CellTiter-Glo detection reagent was added to each well, and luminescence (RLU) was measured. To compare compounds tested in different experiments, we calculate an adjusted raw score (table S1). To calculate the adjusted raw score, we calculated the natural log (ln) of the RLU/1000 for each test compound. Each experiment had a median value for its collection of ln(RLU/1000) scores. The ln(RLU/1000) scores were then slightly adjusted so that each day's experiment had identical median ln(RLU/1000) scores. For example, if 1 day's median score for PQ protection was 1.5 and the next day's test batch had a median score of 1.7, each raw score would be adjusted to give a median of 1.6 on an ln scale. For Fig. 1B, we converted the adjusted raw scores back to RLU/1000 U and then plotted these values as $\log_{10}$.

Cheminformatics and drug-target analyses

Reference compound structures were downloaded from DrugBank in Structure data format (*21*). Analyses of small molecule structures were performed with the ChemmineR package (*22*, *23*). Structure similarity searches of small molecules used atom pairs (*52*) as fragment-based descriptors and the Tanimoto coefficient as similarity metric (*24*, *25*). Analyses of drug-target annotations from DrugBank were performed with the drugbankR package. Target set and drug set enrichment analyses (TSEA and DSEA) used the hypergeometric distribution test along with the Benjamini and Hochberg method for adjusting *P* values for multiple testing implemented by the clusterProfiler package (*26*). Custom R functions were used for generating compound-to-KEGG pathway mappings.

Cell preparation for RNA-seq and RPPA

For RNA-seq, 0.5×10^6 cells were added to each of four wells in a six-well plate per sample. Total volume per well was 3 ml (day 1). Cells were left to adhere overnight. On day 2, the compounds were added to the cells, and the cells were left to incubate overnight. On day 3, medium was removed; cells were washed two times with phosphate-buffered saline (PBS). RNazol was then added directly to the cells and collected for RNA-seq analysis. For RPPA, 10^6 cells were added to one T175 cm^2 flask for each sample. Total volume per flask was 20 ml (day 1). Cells were left to adhere overnight. On day 2, the compounds were added to the cells, and the cells were left to incubate overnight. On day 3, RPPA samples were collected using 0.05% trypsin, trypsin was neutralized after cells detached by adding complete media, and cells were washed twice with PBS. RPPA was performed at the RPPA Core Facility at MD Anderson Cancer Center. Further information about the compounds used in RNA-seq and RPPA is provided in Supplementary Methods, including vendors, catalog numbers, Chemical Abstracts Service numbers, and simplified molecular-input line-entry system structures.

RNA-seq bioinformatics processing

Reads were aligned to mm10 using kallisto v0.43.1. Transcript-level abundances were converted to gene-level count estimates using tximport v1.8.0. Differential expression was calculated using DESeq2 v1.20.0. The data were analyzed through IPA (QIAGEN). To generate hierarchical clustering, Euclidean distances were calculated using the formula $\sqrt{\sum_i (x_i - y_i)^2}$ in R.

Immunoblotting

To assay Nrf2 target expression, MTFs were resuspended in Laemmli sample butter [62.5 mM tris (pH 6.8), 2% SDS, 10% glycerol, 5% BME (beta-Mercaptoethanol), and 1% bromophenol blue]. Samples were sonicated for 30 s on ice, spun down at 4°C for 10 min at 15,000*g*, and the supernatant was collected for protein quantification using a DC protein assay (Bio-Rad, no. 5000112). Samples were boiled, resolved by SDS–polyacrylamide gel electrophoresis, and transferred to polyvinylidene difluoride overnight at 4°C using the Bio-Rad Criterion system. Membranes were stained with Ponceau S, rinsed, and then blocked using 5% milk in TBST (tris-buffered saline/0.1% Tween 20) at room temperature for 1 hour. Primary antibodies [SDHA (Succinate dehydrogenase complex, subunit A), Abcam, ab14715; proliferating cell nuclear antigen (PCNA), ab29; GCLC, ab190685; GCLM, ab 126704; Hmox1, Invitrogen, MA1-112] were diluted in 5% BSA in TBST and incubated with the blot overnight at 4°C with gentle rocking. Secondary incubation was performed at room temperature for 1 hour using either mouse or rabbit secondary antibodies as appropriate (Jackson ImmunoResearch, 115-035-062 or 111-035-045) diluted 1:10,000 in 5% milk in TBST. For detection, blots were immersed in chemiluminescent horseradish peroxidase substrate (Millipore P90720) and imaged using a GE ImageQuant LAS 4000.

C. elegans PQ survival assays

Eggs from N2 worms were transferred to plates seeded with heat-killed bacteria and either DMSO control or 100 μM the indicated drugs (the same dose as used as the high dose in longevity assays). The worms were transferred every day after day 1 of adulthood to separate them from their progeny until day 5 of adulthood. Worms were then transferred to 24-well plates and soaked in 100 mM PQ. Worms were checked every 4 hours for their viability. The experiments in Fig. 6 (A and C) were both performed twice, with 60 worms per assay. Survival curves for each trial were compared by log-rank test; data and analysis on pooled trials are shown. Cox regression was performed using the Cox regression function (coxph) of the package "survival" in R. The test for appropriateness of the assumptions was conducted using the cox.zph() function in the same package. Analysis on pooled data is shown.

SUPPLEMENTARY MATERIALS

Supplementary material for this article is available at http://advances.sciencemag.org/cgi/content/full/6/40/eaaz7628/DC1

View/request a protocol for this paper from *Bio-protocol*.

REFERENCES AND NOTES

1. V. D. Longo, A. Antebi, A. Bartke, N. Barzilai, H. M. Brown-Borg, C. Caruso, T. J. Curiel, R. de Cabo, C. Franceschi, D. Gems, D. K. Ingram, T. E. Johnson, B. K. Kennedy, C. Kenyon, S. Klein, J. J. Kopchick, G. Lepperdinger, F. Madeo, M. G. Mirisola, J. R. Mitchell, G. Passarino, K. L. Rudolph, J. M. Sedivy, G. S. Shadel, D. A. Sinclair, S. R. Spindler, Y. Suh, J. Vijg, M. Vinciguerra, L. Fontana, Interventions to slow aging in humans: Are we ready? *Aging Cell* **14**, 497–510 (2015).

2. D. B. Lombard, R. A. Miller, in *Annual Review of Gerontology*, R. L. Sprott, Ed. (Springer, 2014), vol. 34, pp. 93–138.
3. M. Petrascheck, X. Ye, L. B. Buck, An antidepressant that extends lifespan in adult *Caenorhabditis elegans*. *Nature* **450**, 553–556 (2007).
4. K. Evason, C. Huang, I. Yamben, D. F. Covey, K. Kornfeld, Anticonvulsant medications extend worm lifespan. *Science* **307**, 258–262 (2005).
5. S. Kumar, N. Dietrich, K. Kornfeld, Angiotensin converting enzyme (ACE) inhibitor extends *Caenorhabditis elegans* lifespan. *PLOS Genet.* **12**, e1005866 (2016).
6. X. Ye, J. M. Linton, N. J. Schork, L. B. Buck, M. Petrascheck, A pharmacological network for lifespan extension in *Caenorhabditis elegans*. *Aging Cell* **13**, 206–215 (2014).
7. S. Calvert, R. Tacutu, S. Sharifi, R. Teixeira, P. Ghosh, J. P. de Magalhães, A network pharmacology approach reveals new candidate caloric restriction mimetics in *C. elegans*. *Aging Cell* **15**, 256–266 (2016).
8. T. W. Snell, R. K. Johnston, B. Srinivasan, H. Zhou, M. Gao, J. Skolnick, Repurposing FDA-approved drugs for anti-aging therapies. *Biogerontology* **17**, 907–920 (2016).
9. R. A. Miller, Cell stress and aging: New emphasis on multiplex resistance mechanisms. *J. Gerontol. A Biol. Sci. Med. Sci.* **64**, 179–182 (2009).
10. J. M. Harper, A. B. Salmon, S. F. Leiser, A. T. Galecki, R. A. Miller, Skin-derived fibroblasts from long-lived species are resistant to some, but not all, lethal stresses and to the mitochondrial inhibitor rotenone. *Aging Cell* **6**, 1–13 (2007).
11. A. B. Salmon, S. Murakami, A. Bartke, J. Kopchick, K. Yasumura, R. A. Miller, Fibroblast cell lines from young adult mice of long-lived mutant strains are resistant to multiple forms of stress. *Am. J. Physiol. Endocrinol. Metab.* **289**, E23–E29 (2005).
12. A. M. Pickering, M. Lehr, W. J. Kohler, M. L. Han, R. A. Miller, Fibroblasts from longer-lived species of primates, rodents, bats, carnivores, and birds resist protein damage. *J. Gerontol. A Biol. Sci. Med. Sci.* **70**, 791–799 (2015).
13. K. I. Zhou, Z. Pincus, F. J. Slack, Longevity and stress in *Caenorhabditis elegans*. *Aging (Albany NY)* **3**, 733–753 (2011).
14. Y. Kim, H. Sun, Functional genomic approach to identify novel genes involved in the regulation of oxidative stress resistance and animal lifespan. *Aging Cell* **6**, 489–503 (2007).
15. B. K. Kennedy, N. R. Austriaco Jr., J. Zhang, L. Guarente, Mutation in the silencing gene *SIR4* can delay aging in *S. cerevisiae*. *Cell* **80**, 485–496 (1995).
16. I. Bjedov, J. M. Toivonen, F. Kerr, C. Slack, J. Jacobson, A. Foley, L. Partridge, Mechanisms of lifespan extension by rapamycin in the fruit fly *Drosophila melanogaster*. *Cell Metab.* **11**, 35–46 (2010).
17. J. G. Wood, B. Rogina, S. Lavu, K. Howitz, S. L. Helfand, M. Tatar, D. Sinclair, Sirtuin activators mimic caloric restriction and delay ageing in metazoans. *Nature* **430**, 686–689 (2004).
18. T.-T. Ching, W.-C. Chiang, C.-S. Chen, A.-L. Hsu, Celecoxib extends *C. elegans* lifespan via inhibition of insulin-like signaling but not cyclooxygenase-2 activity. *Aging Cell* **10**, 506–519 (2011).
19. R. H. Houtkooper, L. Mouchiroud, D. Ryu, N. Moullan, E. Katsyuba, G. Knott, R. W. Williams, J. Auwerx, Mitonuclear protein imbalance as a conserved longevity mechanism. *Nature* **497**, 451–457 (2013).
20. E. A. Moehle, K. Shen, A. Dillin, Mitochondrial proteostasis in the context of cellular and organismal health and aging. *J. Biol. Chem.* **294**, 5396–5407 (2019).
21. D. S. Wishart, C. Knox, A. C. Guo, D. Cheng, S. Shrivastava, D. Tzur, B. Gautam, M. Hassanali, DrugBank: A knowledgebase for drugs, drug actions and drug targets. *Nucleic Acids Res.* **36**, D901–D906 (2008).
22. Y. Cao, A. Charisi, L.-C. Cheng, T. Jiang, T. Girke, ChemmineR: A compound mining framework for R. *Bioinformatics* **24**, 1733–1734 (2008).
23. Y. Wang, T. W. H. Backman, K. Horan, T. Girke, fmcsR: Mismatch tolerant maximum common substructure searching in R. *Bioinformatics* **29**, 2792–2794 (2013).
24. T. W. H. Backman, D. S. Evans, T. Girke, Large-scale bioactivity analysis of the small-molecule assayed proteome. *PLOS ONE* **12**, e0171413 (2017).
25. T. W. H. Backman, T. Girke, bioassayR: Cross-target analysis of small molecule bioactivity. *J. Chem. Inf. Model.* **56**, 1237–1242 (2016).
26. G. Yu, L.-G. Wang, G.-R. Yan, Q.-Y. He, DOSE: An R/Bioconductor package for disease ontology semantic and enrichment analysis. *Bioinformatics* **31**, 608–609 (2015).
27. G. Yu, L.-G. Wang, Y. Han, Q.-Y. He, clusterProfiler: An R package for comparing biological themes among gene clusters. *OMICS* **16**, 284–287 (2012).
28. L. M. Schriml, C. Arze, S. Nadendla, Y.-W. W. Chang, M. Mazaitis, V. Felix, G. Feng, W. A. Kibbe, Disease ontology: A backbone for disease semantic integration. *Nucleic Acids Res.* **40**, D940–D946 (2012).
29. M. Kanehisa, S. Goto, M. Hattori, K. F. Aoki-Kinoshita, M. Itoh, S. Kawashima, T. Katayama, M. Araki, M. Hirakawa, From genomics to chemical genomics: New developments in KEGG. *Nucleic Acids Res.* **34**, D354–D357 (2006).
30. M. I. Love, W. Huber, S. Anders, Moderated estimation of fold change and dispersion for RNA-seq data with DESeq2. *Genome Biol.* **15**, 550 (2014).
31. C. Soneson, M. I. Love, M. D. Robinson, Differential analyses for RNA-seq: Transcript-level estimates improve gene-level inferences. *F1000Res* **4**, 1521 (2015).
32. N. L. Bray, H. Pimentel, P. Melsted, L. Pachter, Near-optimal probabilistic RNA-seq quantification. *Nat. Biotechnol.* **34**, 525–527 (2016).
33. A. Subramanian, P. Tamayo, V. K. Mootha, S. Mukherjee, B. L. Ebert, M. A. Gillette, A. Paulovich, S. L. Pomeroy, T. R. Golub, E. S. Lander, J. P. Mesirov, Gene set enrichment analysis: A knowledge-based approach for interpreting genome-wide expression profiles. *Proc. Natl. Acad. Sci. U.S.A.* **102**, 15545–15550 (2005).
34. Q. Ma, Role of nrf2 in oxidative stress and toxicity. *Annu. Rev. Pharmacol. Toxicol.* **53**, 401–426 (2013).
35. A. D. Rouillard, G. W. Gundersen, N. F. Fernandez, Z. Wang, C. D. Monteiro, M. G. McDermott, A. Ma'ayan, The harmonizome: A collection of processed datasets gathered to serve and mine knowledge about genes and proteins. *Database (Oxford)* **2016**, baw100 (2016).
36. T. K. Blackwell, M. J. Steinbaugh, J. M. Hourihan, C. Y. Ewald, M. Isik, SKN-1/Nrf, stress responses, and aging in *Caenorhabditis elegans*. *Free Radic. Biol. Med.* **88**, 290–301 (2015).
37. K. J. Pearson, K. N. Lewis, N. L. Price, J. W. Chang, E. Perez, M. V. Cascajo, K. L. Tamashiro, S. Poosala, A. Csiszar, Z. Ungvari, T. W. Kensler, M. Yamamoto, J. M. Egan, D. L. Longo, D. K. Ingram, P. Navas, R. de Cabo, Nrf2 mediates cancer protection but not prolongevity induced by caloric restriction. *Proc. Natl. Acad. Sci. U.S.A.* **105**, 2325–2330 (2008).
38. R. Strong, R. A. Miller, A. Antebi, C. M. Astle, M. Bogue, M. S. Denzel, E. Fernandez, K. Flurkey, K. L. Hamilton, D. W. Lamming, M. A. Javors, J. P. de Magalhães, P. A. Martinez, J. M. McCord, B. F. Miller, M. Müller, J. F. Nelson, J. Ndukum, G. E. Rainger, A. Richardson, D. M. Sabatini, A. B. Salmon, J. W. Simpkins, W. T. Steegenga, N. L. Nadon, D. E. Harrison, Longer lifespan in male mice treated with a weakly estrogenic agonist, an antioxidant, an α-glucosidase inhibitor or a Nrf2-inducer. *Aging Cell* **15**, 872–884 (2016).
39. C. Tonelli, I. I. C. Chio, D. A. Tuveson, Transcriptional regulation by Nrf2. *Antioxid. Redox Signal.* **29**, 1727–1745 (2018).
40. Y. Meyer, B. B. Buchanan, F. Vignols, J.-P. Reichheld, Thioredoxins and glutaredoxins: Unifying elements in redox biology. *Annu. Rev. Genet.* **43**, 335–367 (2009).
41. S. S. Nishizuka, G. B. Mills, New era of integrated cancer biomarker discovery using reverse-phase protein arrays. *Drug Metab. Pharmacokinet.* **31**, 35–45 (2016).
42. N. Khan, H. Mukhtar, Tea polyphenols in promotion of human health. *Nutrients* **11**, 39 (2018).
43. C. Rajagopal, M. B. Lankadasari, J. M. Aranjani, K. B. Harikumar, Targeting oncogenic transcription factors by polyphenols: A novel approach for cancer therapy. *Pharmacol. Res.* **130**, 273–291 (2018).
44. T. Blanco-Ayala, A. C. Andérica-Romero, J. Pedraza-Chaverri, New insights into antioxidant strategies against paraquat toxicity. *Free Radic. Res.* **48**, 623–640 (2014).
45. E. J. Calabrese, E. Agathokleous, Building biological shields via hormesis. *Trends Pharmacol. Sci.* **40**, 8–10 (2019).
46. S. Peng, Y. Hou, J. Yao, J. Fang, Activation of Nrf2-driven antioxidant enzymes by cardamonin confers neuroprotection of PC12 cells against oxidative damage. *Food Funct.* **8**, 997–1007 (2017).
47. S. F. Leiser, R. A. Miller, Nrf2 signaling, a mechanism for cellular stress resistance in long-lived mice. *Mol. Cell. Biol.* **30**, 871–884 (2010).
48. A. H. Salehi, S. J. Morris, W.-C. Ho, K. M. Dickson, G. Doucet, S. Milutinovic, J. Durkin, J. W. Gillard, P. A. Barker, AEG3482 is an antiapoptotic compound that inhibits Jun kinase activity and cell death through induced expression of heat shock protein 70. *Chem. Biol.* **13**, 213–223 (2006).
49. S. Dayalan Naidu, R. V. Kostov, A. T. Dinkova-Kostova, Transcription factors Hsf1 and Nrf2 engage in crosstalk for cytoprotection. *Trends Pharmacol. Sci.* **36**, 6–14 (2015).
50. Y. Zhang, Y.-H. Ahn, I. J. Benjamin, T. Honda, R. J. Hicks, V. Calabrese, P. A. Cole, A. T. Dinkova-Kostova, HSF1-dependent upregulation of Hsp70 by sulfhydryl-reactive inducers of the KEAP1/NRF2/ARE pathway. *Chem. Biol.* **18**, 1355–1361 (2011).
51. P. Zhang, Y. Zhai, J. Cregg, K. K.-H. Ang, M. Arkin, C. Kenyon, Stress resistance screen in a human primary cell line identifies small molecules that affect aging pathways and extend *Caenorhabditis elegans*' lifespan. *G3 (Bethesda)* **10**, 849–862 (2020).
52. X. Chen, C. H. Reynolds, Performance of similarity measures in 2D fragment-based similarity searching: Comparison of structural descriptors and similarity coefficients. *J. Chem. Inf. Comput. Sci.* **42**, 1407–1414 (2002).
53. N. J. Linford, C. Bilgir, J. Ro, S. D. Pletcher, Measurement of lifespan in *Drosophila melanogaster*. *J. Vis. Exp.* , 50068 (2013).
54. D. Garigan, A.-L. Hsu, A. G. Fraser, R. S. Kamath, J. Ahringer, C. Kenyon, Genetic analysis of tissue aging in *Caenorhabditis elegans*: A role for heat-shock factor and bacterial proliferation. *Genetics* **161**, 1101–1112 (2002).
55. S. Brenner, The genetics of *Caenorhabditis elegans*. *Genetics* **77**, 71–94 (1974).

Acknowledgments: We thank M. Petrascheck and M. Truttmann for discussions. Some studies reported in this publication were carried out at the Center for Chemical Genomics (CCG) at the University of Michigan Life Sciences Institute. **Funding:** This work was supported by the Glenn Foundation for Medical Research. A.H.G. was supported by T32 GM113900 and T32 AG000114. We would also like to cite the following grants: R01GM101171 and R01HL114858 (to D.B.L.); R01AG030593 and R01AG051649 (to S.D.P.); and U24AG051129, 1S10-OD016290-01A1, and NSF award ABI-1661152 (to T.G.). **Author contributions:** Study conception: D.B.L., A.-L.H., S.D.P., and R.A.M. Data analysis and interpretation: D.B.L., A.H.G., C.G., T.-T.C., Z.N.-C., T.G., A.-L.H., S.D.P., and R.A.M. Data collection: W.J.K., A.H.G. C.G., M.H., W.D., Y.L. T.-T.C., F.-Y.W., T.S.C., Y.D., and T.G. Wrote the manuscript: D.B.L. **Competing interests:** The authors declare that they have no competing interests. **Data and materials availability:** RNA-seq results have been deposited at GEO, accession number GSE130294. All data needed to evaluate the conclusions of the paper are present in the paper and/or the Supplementary Materials. Additional data related to this paper may be requested from the authors.

Submitted 7 October 2019
Accepted 14 August 2020
Published 2 October 2020
10.1126/sciadv.aaz7628

Citation: D. B. Lombard, W. J. Kohler, A. H. Guo, C. Gendron, M. Han, W. Ding, Y. Lyu, T.-T. Ching, F.-Y. Wang, T. S. Chakraborty, Z. Nikolovska-Coleska, Y. Duan, T. Girke, A.-L. Hsu, S. D. Pletcher, R. A. Miller, High-throughput small molecule screening reveals Nrf2-dependent and -independent pathways of cellular stress resistance. *Sci. Adv.* **6**, eaaz7628 (2020).

Science Advances

High-throughput small molecule screening reveals Nrf2-dependent and -independent pathways of cellular stress resistance

David B. Lombard, William J. Kohler, Angela H. Guo, Christi Gendron, Melissa Han, Weiqiao Ding, Yang Lyu, Tsui-Ting Ching, Feng-Yung Wang, Tuhin S. Chakraborty, Zaneta Nikolovska-Coleska, Yuzhu Duan, Thomas Girke, Ao-Lin Hsu, Scott D. Pletcher and Richard A. Miller

Sci Adv **6** (40), eaaz7628.
DOI: 10.1126/sciadv.aaz7628